THE JOURNAL OF PHYSICAL CHEMISTRY C

Article

pubs.acs.org/JPCC

Thermodynamics and Characteristics of Heterogeneous Nucleation on Fractal Surfaces

Qiang Zeng* and Shilang Xu

Institute of Advanced Engineering Structures and Materials, College of Civil Engineering and Architecture, Zhejiang University, Yuhangtang Rd 866, 310058, Hangzhou, P.R. China

ABSTRACT: Clarifying heterogeneous nucleation process on fractal surfaces is an important issue to understand its thermodynamic principles and forward the engineering aspects. We developed a thermodynamic model to capture the process of forming a crystal or drop embryo on fractal surfaces and the corresponding characteristic parameters. We showed that the differences between the critical size of the embryos on the fractal surfaces and those on the flat surfaces are negligible for the hydrophobic nuclei, but become significant for the hydrophilic nuclei. We reported the available domains of forming the critical embryos and obtained the shape function for the first time. The results also recover the data reported in the literature. Finally, we present the possible mechanisms of vanishing of the energy barriers against forming the critical embryos on the fractal surfaces as the apparent contact angle is relatively small. The obtained results may help to engineer the nucleation process by designing substrate surfaces in a fractal structure.

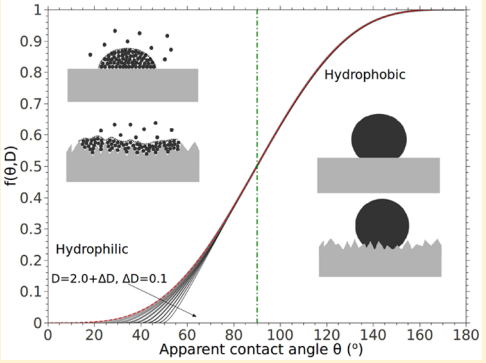

INTRODUCTION

The ability to control heterogeneous nucleation with auxiliaries is of significant importance and has clear engineering applications, such as in the development of ice-phobic surfaces,[1−3] the prevention of ice accretion and adhesion on surfaces against material damages,[4,5] and the selection and control of protein crystals.[6−8] Therefore, understanding the nucleation mechanisms of a phase on a foreign surface and the technology development for further applications are desirable and has been the subject of considerable attention.[8−19]

It is known that introduction of a foreign surface can facilitate or delay nucleation to form crystals or to condense droplets on the surface. One of the most important factors for the process is the surface topography. For example, Holbrough et al.[20] observed that the nucleation density can be significantly increased as the mica surfaces were scratched by grits with the larger size, and also indicated that surface topography is an important factor that is possible for an enhancement of nucleation, and that the engineering nanoscale topographical features could potentially control heterogeneous nucleation. Similar observations are extensive.[8,15,16,21] However, recent molecular dynamics simulations by Zhang et al.[22] argued that the nucleation promotion ability of the rough surfaces is associated with the surface structures. Their findings showed that the nucleation can be promoted remarkably only when the characteristic length of the surface structure matches well with the size of the crystal, and this kind of promotion disappears and the nucleation rate is even smaller than that on the smooth surface if the geometry match between the surface and the crystal is poor. Campbell et al.[23] also argued the preferred nucleation effects by roughing surfaces based on a study of the freezing of 50 μm diameter water drops on silicon, glass, and mica substrates roughened by scratching with diamond powders of different size distributions. We must note that the above-mentioned debates are based on the artificial surfaces whose roughness is controlled in the tests. For the surfaces of materials without specific alterations that show fractal properties (e.g., porous silica,[7,24−26] cement-based porous materials,[27,28] and fractured metal surfaces[16]), the relevant research is rather insufficient. A fractal surface shows feature of self-similarity or exhibits a repeating pattern that displays at every scale. Generally, the nature of self-similarity allows expression of the number of the measuring element, N, with size r as follows,[29]

$$N \propto r^{D} \tag{1}$$

where D is the fractal dimension.

On the basis of the fractal structure of the surfaces and the thermodynamic principles of heterogeneous nucleation, much research has been done to deepen the understanding of nucleation on the fractal surfaces.[7,14,16,24,25,30,31] This has shown that the number of adsorbed molecules or nucleation seeds on a fragment with a fractal surface significantly exceeds that on one with flat surfaces.[7,16,24] The conclusion is reasonable as the fractal surface provides more areas to accommodate the nuclei. Moreover, the rough fractal surface could change the apparent contact angle between the crystal and the substrate, which would result in changing the energy for forming nuclei on the fractal surface, and thus influencing the heterogeneous nucleation process. References 14 and 31

Received: August 8, 2015
Revised: November 9, 2015
Published: November 11, 2015

DOI: 10.1021/acs.jpcc.5b07709
J. Phys. Chem. C 2015, 119, 27426−27433

have noticed the characteristics of the apparent contact angle between the nucleus and the fractal surface, but have not shown thermodynamic formulas to characterize the critical size of the nuclei in contact with the very fractal surface and the required energy against the energy barriers of forming nuclei. Therefore, lacking is an integral thermodynamic model and parameters that are able to characterize the heterogeneous nucleation process, and help to understand how the fractal structure of the surface influences the nucleation process.

In this work, to develop the thermodynamic model of heterogeneous nucleation on fractal surfaces, we examined the change of free energy as the nucleation process takes place, and for the first time present the formulas of the critical size of the nucleation embryos and the shape function (following the concept of Fletcher's shape function) to the apparent contact angle and fractal dimension explicitly, to the best knowledge of the authors. We then analyzed the parameters that are featured and distinct from the classic nucleation on flat surfaces. We also proposed a mechanism that is possible to explain the abnormality of the shape function in the regions of low apparent contact angles. The results may help to engineer the nucleation process by selecting or fabricating appropriate fractal surfaces, for example, using porous silica surface to promote nucleation rates of proteins.

THEORY BACKGROUND AND THERMODYNAMICAL FORMULATION

We start the formulation section from the free energy changes ΔG as a nucleus is formed and in contact with or a droplet is condensed on a rough surface; see Figure 1. We assume that

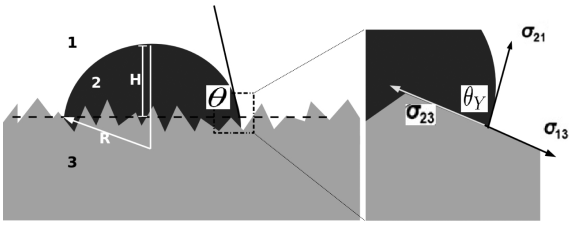

Figure 1. Schematic illustration of a nucleus in contact with a rough surface and the relationship between the apparent contact angle, θ, and the Young contact angle, θ_Y.

the contacted areas of the surfaces are completely covered by the nuclei without empty voids involved, so the Wenzel-type contact angle interpretation is used. The cases of typical hydrophobic surfaces that may show incomplete contact with the nuclei or drops and thus have empty voids between the phases (described by the Cassie–Baxter-type contact angle interpretation) are not considered and are beyond the scope of this study. As suggested in ref 32, the real crystal–substrate (or liquid–solid for wetting) interfacial configuration is more likely to be a mix between the Cassie–Baxter state, occurring at the larger scales, and the Wenzel state at the smaller scales. The assumptions are reasonable given that the nuclei are generally very small (in the magnitude of nanometer). We also assume that the theoretical equations hold independent of the size of the nuclei, pores, and substrates, although debates of the relevant issues (e.g., the available range and physical limitation of the Wenzel model[33−38]) have been extensively conducted in the literature.

We shall assume that the pressure of the parent phase that is generally vapor (or liquid) is uniform and does not change as nucleation takes places, and there is no mass transport in and/or out of the system. To follow classic nucleation theory, we adopted the constraints used by Fletcher[9] who believed that the application of macroscopic concepts like surface free energy to very small groups of molecules is acceptable, although the thermodynamic properties may deviate from their macroscopic values (e.g., ref 39), but of which the extent is relatively small when supercooling or supersaturation is insignificant. Note that the assumptions may be debatable as the line tension effect may arise for very small nuclei or droplets that are highly curved.[40] Also the curvature effect tends to alter the free energy expression of the system (see for instance the work by Ward and co-workers[41−43]), but we shall have to neglect its effects in the present discussion because the results in the present study require comparison with those in the literature, and the relevant issues may provide further investigation incentives in the future.

According to classic nucleation theory, the change in the free energy, ΔG, accompanying the nucleation, can be expressed by

$$\Delta G = \Delta G_v V_2 + \sigma_{12}A_{12} + (\sigma_{23} - \sigma_{13})A_{23} \tag{2}$$

where the subscripts 1, 2, and 3 refer to the parent phase, nucleation embryo or germ, and solid substrate, respectively, ΔG_v is the free energy change per unit volume of the embryo from phase 1 to phase 2, V_2 is the volume of the embryo, σ_{ij} is the interfacial energy between phases i and j, and A_{ij} is the corresponding interfacial area. Equation 2 indicates that the free energy change, ΔG, is composed of the (volumetric) energy change of bulk phase transition, $\Delta G_v V_2$, and the possible energy change as surfaces are created, $\sigma_{12}A_{12}$, eliminated, $-\sigma_{13}A_{23}$, and replaced by the new interface, $\sigma_{23}A_{23}$.

When a spherical-cap embryo of radius R on a rough surface is considered (as illustrated in Figure 1), the volume of the embryo, V_2, the area of the created interface between the parent phase 1 and the embryo phase 2, A_{12}, and the area of the eliminated interface between the parent phase 1 and the substrate phase 3, which is replaced by the interface between the embryo phase 2 and the substrate phase 3, $\sigma_{23}A_{23}$, can be given by

$$V_2 = \frac{R^3\pi}{3}(2 - 3\cos\theta + \cos^3\theta) \tag{3a}$$

$$A_{12} = 2\pi R^2(1 - \cos\theta) \tag{3b}$$

$$A_{23} = \pi R^2 \sin^2 3\theta\phi \tag{3c}$$

where θ is the apparent contact angle between the embryo phase 2 and the substrate phase 3, and ϕ is a roughness ratio that indicates the surface roughness of the substrate compared with the smooth planar surface. In eq 3, we also assume the apparent contact angle of an embryo on an ideal rough surface that is homogeneous and has a negligible body force, line tension, or contact angle hysteresis between the embryo phase 2 and the substrate phase 3. We shall note the differences between the apparent contact angle, θ, and the *real* or *intrinsic* contact angle, θ_Y (or the Young contact angle), between the embryo phase 2 and the substrate phase 3, which gives

$$\sigma_{12}\cos\theta_Y = \frac{\sigma_{12}\cos\theta}{\phi} = (\sigma_{13} - \sigma_{23}) \tag{4}$$

Equation 4 shows the relationship between the Young contact angle and the apparent contact angle, and how the surface

DOI: 10.1021/acs.jpcc.5b07709
J. Phys. Chem. C 2015, 119, 27426−27433

roughness influences the apparent contact angle. Equation 4 is also known as the Wenzel equation.

Generally, for a substrate with rough surface that is homogeneous in geometry and physical properties (or chemical composites), ϕ = const. However, for a fractal rough surface the roughness ratio, ϕ, is a function of the projected length, $R \sin\theta$, the low boundary of length with fractal measurement of the surface, L_l, and the fractal dimension, D, which gives[14]

$$\phi = \left(\frac{2R\sin\theta}{L_l}\right)^{(D-2)}, \quad L_l < 2R\sin\theta < L_u \tag{5}$$

where L_u is the upper bound of length with fractal measurement of the surface. We emphasize that eq 5 holds in the region of $L_l < 2R\sin\theta < L_u$, because nucleation embryos are generally very small. If a large nucleus or droplet is considered, for example, the spherical-cap solution drops with diameter of around 1 mm placed on the fractal surfaces for contact angle measurement,[44−46] a relationship of $\phi = (L_u/L_l)^{(D-2)}$, $L_u < 2R\sin\theta$[47] should be used to replace eq 5. Substitution of eq 5 into eqs 4 and (3c), one has

$$\cos\theta = \cos\theta_Y\left(\frac{2R\sin\theta}{L_l}\right)^{(D-2)} \tag{6}$$

and

$$A_{23} = \pi(R\sin\theta)^2\left(\frac{2R\sin\theta}{L_l}\right)^{(D-2)} \tag{7}$$

It can be seen from eq 6 that for a nucleation process taking place on a fractal surface, the apparent contact angle depends on the intrinsic wetting angle, the ratio of the radius of the contact circle to the low boundary of length with fractal measurement, and the fractal dimension of the substrate surface (cf. the constant roughness ratio of the sawtooth surfaces[48]), and so does the area of the interface between the embryo phase 2 and the substrate phase 3 as seen from eq 7. This yields a distinct feature of nucleation on fractal surfaces other than that on smooth surfaces: the apparent contact angle is size-dependent, that is, $\theta = \theta(R)$. Differential operation on eq 5 yields

$$\frac{\partial\theta(R)}{\partial R} = -\frac{1}{R}\frac{(D-2)\cos\theta\sin\theta}{(D-2)\cos^2\theta + \sin^2\theta} \tag{8}$$

In eq 8, the radius of the spherical-cap embryo, R, and the low boundary of length with fractal measurement of the surface, L_l, do not appear, indicating that the changing rates of the apparent contact angle against the embryo size is independent of L_l. This could eliminate the possible scale problems of the real surfaces of a material when pursuing the critical embryo size (see the following text).

According to classic nucleation theory and maintaining the concept of the apparent contact angle, the change in the free energy for nucleation formation on a fractal surface can be expressed as an elegant equation given by

$$\Delta G = \left(\frac{\pi R^3}{3}\Delta G_v + \pi R^2\sigma_{12}\right)(2 - 3\cos\theta + \cos^3\theta) \tag{9}$$

Equation 9 is exactly the same with the expression of ΔG formulated for nucleation on a smooth planar surface. Similarly, to determine the critical embryo radius R_c from eq 9, a differential operation on ΔG to R is conducted. This yields

$$\frac{\partial\Delta G}{\partial R} = \pi R(R\Delta G_v + 2\sigma_{12})(2 - 3\cos\theta + \cos^3\theta) + \pi R^2(R\Delta G_v + 3\sigma_{12})\sin^3\theta\frac{\partial\theta(R)}{\partial R} \tag{10}$$

Substitution of eq 8 into eq 10, and use of the requirement of $\partial\Delta G/\partial R = 0$, one has

$$g(\theta, D)R\Delta G_v + s(\theta, D)2\sigma = 0 \tag{11}$$

where $g(\theta, D)$ and $s(\theta, D)$ are the functions that only depend on the fractal dimension and apparent contact angle,

$$g(\theta, D) = \sum_{i=0}^{N} Bg_i(D)\cos^i\theta \tag{12a}$$

$$s(\theta, D) = \sum_{i=0}^{N} Bs_i(D)\cos^i\theta \tag{12b}$$

where $Bg_i(D)$ and $Bs_i(D)$ are the coefficients of the polynomial functions of cos θ governed by the fractal dimension, D. The expressions of $Bg_i(D)$ and $Bs_i(D)$ are present in Table 1.

Table 1. Expressions for $Bs_i(D)$, $Bg_i(D)$ and $Bp_i(D)$

i	$Bs_i(D)$	$Bg_i(D)$	$Bp_i(D)$
0	2	2	$-2D + 2$
1	$-3D/2$	$-D - 1$	$-3D + 9$
2	$2(D - 3)$	$2(D - 3)$	$2D^2 - 1$
3	4	$-D + 6$	$-9D^2 + 41D - 53$
4	0	0	$8D^2 - 38D + 42$
5	$-D/2$	-1	$D^2 - 9D + 19$
6	0	0	0
7	0	0	$-2D^2 + 11D - 15$

From eq 11, one obtains an expression of the critical embryo size against the fractal dimension and apparent contact angle given by

$$R_c = R_{c0}h(\theta, D) \tag{13}$$

where R_{c0} is the critical embryo size in some special geometric conditions, for example, the spherical embryos by homogeneous nucleation, the spherical-cap embryos in contact with the smooth planar surfaces and concave and convex surfaces,[9,11,13] and $R_{c0} = -2\sigma_{12}/\Delta G_v$, and $h(\theta, D)$ is a coefficient of critical size that inflects the matching extent or derivation extent between R_c and R_{c0},

$$h(\theta, D) = [s(\theta, D)]/[g(\theta, D)] = \left[2 - \frac{3}{2}D\cos\theta + 2(D-3)\cos^2\theta + 4\cos^3\theta - \frac{D}{2}\cos^5\theta\right]/[2 - (D+1)\cos\theta + 2(D-3)\cos^2\theta + (6-D)\cos^3\theta - \cos^5\theta] \tag{14}$$

When $D = 2$, or $\theta = \pi/2$, then $h(\theta, D) = 1$, so $R_c = R_{c0} = -2\sigma_{12}/\Delta G_v$.

Differentiating eq 10 with respect to R and subsuming $R = R_c$, we have

DOI: 10.1021/acs.jpcc.5b07709
J. Phys. Chem. C 2015, 119, 27426−27433

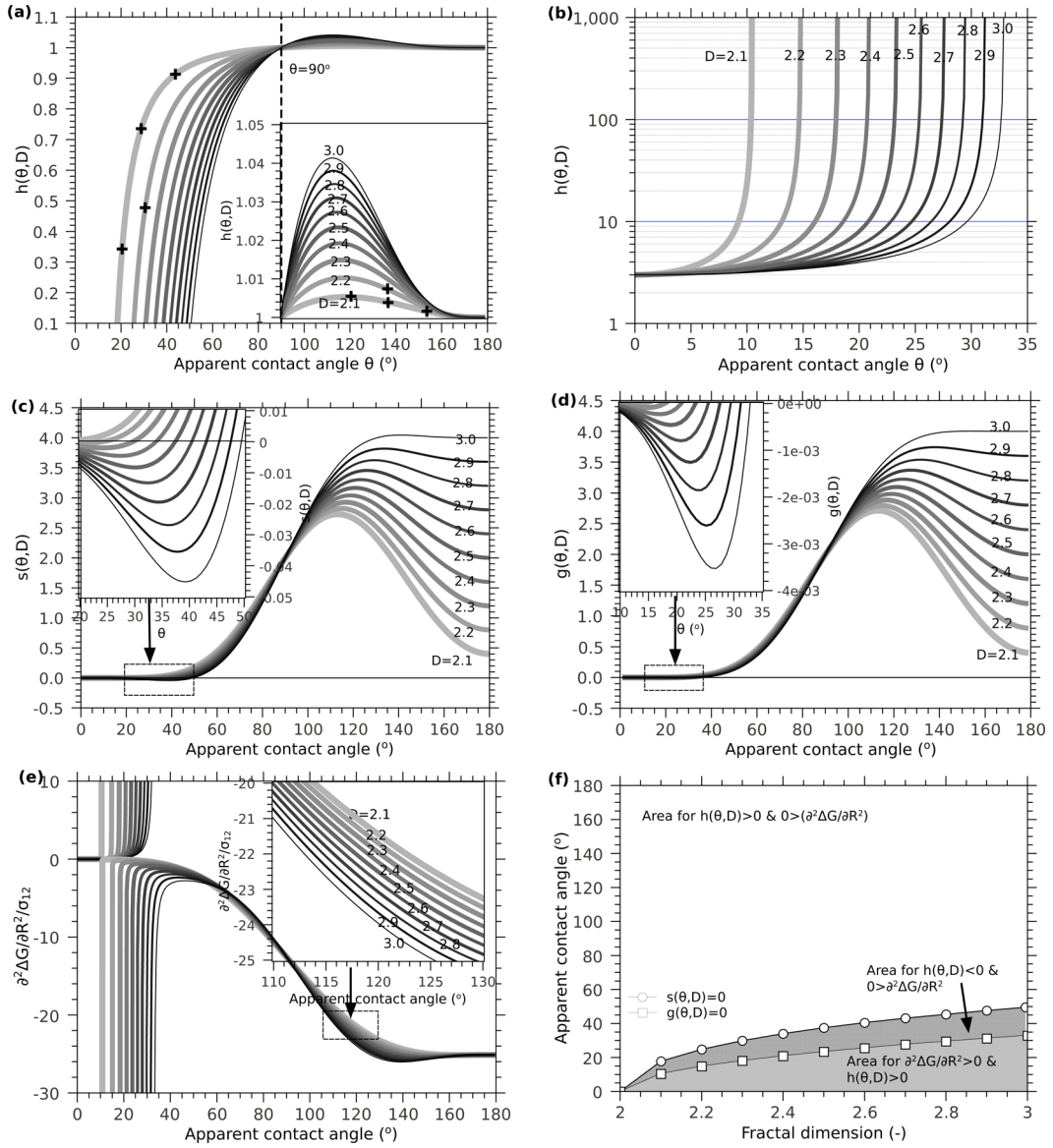

Figure 2. Plots of $h(\theta, D)$ with $h(\theta, D) > 0$ in (a) the regions of moderate and large apparent contact angles and (b) the regions of small apparent contact angles with different fractal dimensions. Plots of (c) $s(\theta, D)$ and (d) $g(\theta, D)$ against θ with different fractal dimensions. (e) Plots of $\partial^2\Delta G/\partial R^2|_{R=R_c}/\sigma_{12}$ against θ with different fractal dimensions and (f) the domains under different conditions. The crosses in the subfigure (a) represent the data from ref 14.

$$\left.\frac{\partial^2\Delta G}{\partial R^2}\right|_{R=R_c} = 2\pi\sigma_{13}[1 - 2h(\theta, D)](2 - 3\cos\theta + \cos^3\theta) + 2\pi\sigma_{13}[1 - h(\theta, D)]\frac{\sum_{i=0}^{N} Bp_i(D)\cos^i\theta}{[(D-2)\cos^2\theta + \sin^2\theta]^2} \quad (15)$$

where $Bp_i(D)$ represents the coefficients of the polynomial function of cos θ that is only depending on the fractal dimension, D; see Table 1 for the detailed expressions.

Substituting eq 13 into eq 9, we can obtain the change in the free energy with the critical embryo size, $\Delta G^*(R = R_c)$, in the following form,

$$\Delta G^*|_{R=R_c} = \frac{16\pi}{3}\frac{{\sigma_{12}}^3}{{\Delta G_v}^2} f(\theta, D) \quad (16)$$

where $f(\theta, D)$ can be cataloged as a shape function following the concept of Fletcher[9] and can be expressed as

$$f(\theta, D) = \frac{1}{4}[3h^2(\theta, D) - 2h^3(\theta, D)](2 - 3\cos\theta + \cos^3\theta) \quad (17)$$

Note that eq 17 is physically different with the shape functions given by Fletcher,[9] Liu,[10] and Qian and Ma[11,13] because the geometric features of the substrate surfaces are different. The analysis given below details how the fractal dimension and apparent contact angle will affect the nucleation process.

RESULTS AND DISCUSSION

Critical Size and Available Domain. Since R_{c0} is an intrinsic quantity as an embryo forms homogeneously or heterogeneously in contact with a nonfractal surface, the most representative characteristic parameter for the process of

DOI: 10.1021/acs.jpcc.5b07709
J. Phys. Chem. C 2015, 119, 27426−27433

nucleation on a fractal surface could be the coefficient of critical size, $h(\theta, D)$. Figure 2a shows the values of $h(\theta, D)$ against θ at different fractal dimensions. As is seen, $h(\theta, D)$ shows completely different values between the regions of $\theta \in [0°, 90°)$ and $\theta \in [90°, 180°)$. When the apparent contact angle is right and obtuse, i.e., $\theta \in [90°, 180°)$, the values of $h(\theta, D)$ have no significant differences with 1. In other words, the deviation extent between R_c and R_{c0} is minor, that is, $|R_c - R_{c0}|/R_{c0} < 5\%$; see the enlarged portion of $\theta \in [90°, 180°)$ in Figure 2a. A maximum deviation appears around 110°, and the extent increases with the fractal dimension increasing. For example, as D increases from 2.1 to 3, the maximum deviation increases from 0.5% to 4.2%. When the apparent contact angle is larger than 160°, the curves of $h(\theta, D)$ with different fractal dimensions almost collapse together. This suggests, for the very hydrophobic surfaces, the fractal dimension has almost no influence on the critical nucleation embryo size. When the apparent contact angle is acute, that is, $\theta \in [0°, 90°)$, each individual curve of $h(\theta, D)$ with a predetermined fractal dimension deviates with 1 progressively as θ decreases from 90° to a value with which $h(\theta, D) = 0$. Then a singularity of $h(\theta, D)$ appears when θ decreases to a lower value, and after that the relationship of $h(\theta, D) > 0$ holds again. Figure 2b shows the curves of $h(\theta, D) > 0$ with θ in the very first apparent contact angle regions. As is shown, in those regions, $h(\theta, D)$ increases from 3 to an infinity value as θ increases from 0 to a certain value for a given fractal dimension.

The values and signs of $h(\theta, D)$, as aforementioned, are resulted from a fraction with the numerator, $s(\theta, D)$, and the denominator, $g(\theta, D)$; see eq 14. Figure 2c,d shows the plots of $s(\theta, D)$ and $g(\theta, D)$ against the apparent contact angle with different fractal dimensions. From the figure, we find that both the numerator, $s(\theta, D)$, and the denominator, $g(\theta, D)$, display similar curves with the same fractal dimension, but present minor differences in the regions of relatively small apparent contact angles. Magnified plots of Figure 2c,d show that both $s(\theta, D)$ and $g(\theta, D)$ are negative, and the domains for $s(\theta, D) < 0$ are bigger than the ones for $g(\theta, D) < 0$. So the domains of $h(\theta, D) > 0$ in the regions of relatively small apparent contact angles illustrated in Figure 2b must conform to the requirements of $s(\theta, D) < 0$ and $g(\theta, D) < 0$, and the singularities of $h(\theta, D)$ appear as $g(\theta, D) = 0$. For the cases of $s(\theta, D) = 0$ and $g(\theta, D) = 0$, the corresponding apparent contact angles increase with the fractal dimensions increasing; see the open symbols and solid lines displayed in Figure 2f.

It is noteworthy that the requirement of $h(\theta, D) > 0$ is not sufficient to conclude the validity of the domains where nucleation with the critical embryos takes place. Instead, to define the critical embryo radius, R_c, from eq 9, the conditions of both $\partial\Delta G/\partial R = 0$ and $\partial^2\Delta G/\partial R^2 < 0$ must be satisfied.[9,13] Figure 2e displays the curves of $\partial^2\Delta G/\partial R^2|_{R=R_c}/\sigma_{12}$ against the apparent contact angle as the fractal dimension changes from 2.1 to 3. Clearly, in the domains where $g(\theta, D) < 0$, $\partial^2\Delta G/\partial R^2|_{R=R_c} > 0$, saying that the physical requirements for heterogeneous nucleation in the critical embryo size are not satisfied, although $h(\theta, D) > 0$ as depicted in Figure 2b. So the available domain of $h(\theta, D)$ should be the area where both the relationships of $h(\theta, D) > 0$ and $\partial^2\Delta G/\partial R^2|_{R=R_c} < 0$ always hold, as shown in Figure 2f.

Shape Function. A distinct feature noted from this development is that the apparent contact angle between the embryo phase 2 and the substrate phase 3 changes with the embryo size, R, and so does the roughness ratio; see eq 6. This relationship would not hold for any other geometric surfaces. And this feature leads to the very distinct critical embryo size coefficient, $h(\theta, D)$, as aforementioned, and influences the shape function, $f(\theta, D)$, that indicates the deviation of the heterogeneous nucleation process from the homogeneous nucleation process. Figure 3a shows the plots of $f(\theta, D)$

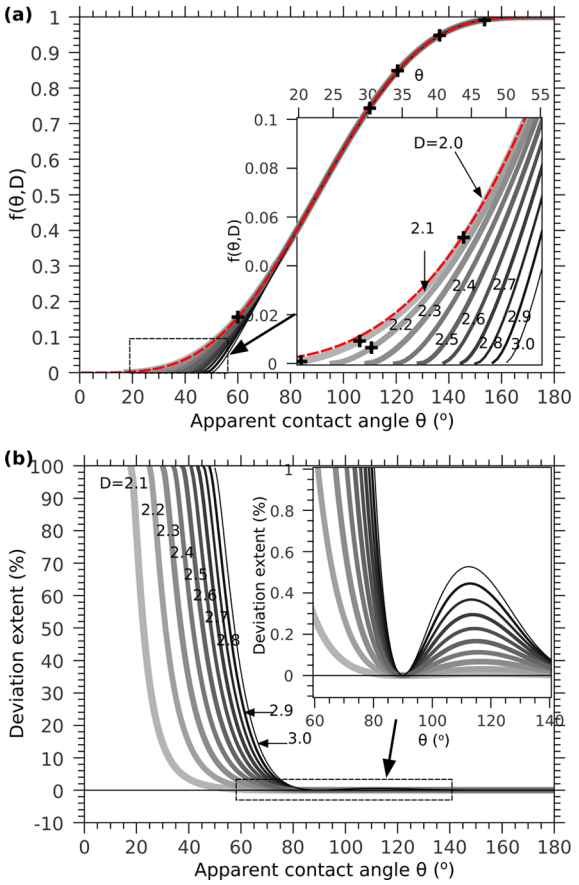

Figure 3. (a) Plots of $f(\theta, D)$ against θ as fractal dimension changes from 2 to 3 and (b) deviation extents of $f(\theta, D)$ between the fractal and smooth surfaces. The plus signs represent the data from ref 14.

against θ with different fractal dimensions. For comparison, the shape factor for nucleation on flat surfaces with different wettabilities, $f(\theta, 2) = (2 - 3\cos\theta + \cos^3\theta)/4$, is superimposed. We find that the difference between the shape function with fractal $(D > 2)$ and smooth $(D = 2)$ surfaces occurs primarily in the regions of relatively small or moderate apparent contact angles, that is , $\theta < 80°$, and diminishes rapidly as $\theta > 80°$, as is demonstrated by the deviation extent, $|f(\theta, D) - f(\theta, 2)|/f(\theta, 2) \times 100\%$, depicted in Figure 3b. Small perturbation of the deviation extent occurs in the region of $\theta \in (90, 140)°$, following the deviation extent between R_c and R_{c0} shown in Figure 2a. The results imply that, in the region of relatively large apparent contact angles, the shape function of heterogeneous nucleation on fractal surface is almost the same as that on smooth surface regardless of the fractal dimension.

Small contact angles favor nucleation owing to the fact that the required free energy for forming a nucleus is lowered. This is also clear from Figure 3a where $f(\theta, D)$ always decreases with decreasing θ, irrespective of the fractal dimension D. Again, the available domain for $f(\theta, D)$ should follow those for forming

DOI: 10.1021/acs.jpcc.5b07709
J. Phys. Chem. C 2015, 119, 27426−27433

critical embryos during nucleation depicted in Figure 2f. This says the energy barrier resistance against forming nuclei in critical size on a fractal surface could reduce to zero as θ decreases to a certain value. In other words, nucleation on a fractal surface takes place spontaneously as θ is relatively small. According to eq 17, θ, with which $h(\theta, D) = 0$ or $s(\theta, D) = 0$, also leads to $f(\theta, D) = 0$, so the occurrence of spontaneous nucleation on a fractal surface is appearing when θ is in the area below the curve of $s(\theta, D) = 0$ in Figure 2f. This distinguishes the heterogeneous nucleation taking place on fractal surfaces from that on smooth surfaces or other conditioned surfaces presented in refs 11 and 13. Figure 3, together with Figure 2, presents the characteristics of heterogeneous nucleation on fractal surfaces.

Comparison with the Literature. Previous study by Wang et al.[14] has forwarded the analysis of heterogeneous nucleation on fractal surfaces and discussed the potent influential factors, for example, the fractal dimension and the intrinsic wetting angle, and some obtained results in the exemplified cases. As a matter of fact, the results in ref 14 can be the specific cases of our general model developed in this study. For comparison, the results of $h(\theta, D)$ and $f(\theta, D)$ in ref 14 are superimposed in Figure 2a and Figure 3a, respectively. On the basis of the results from the analysis, Wang et al. found the increase of the critical nucleus radius and nucleation energy with the fractal dimensions increasing for a nonwetting nucleus on the fractal surface, and the opposite tendency for a wetting nucleus on the same substrate surface. However, the authors did not give the general expressions for critical embryo size, eq 14, shape function, eq 17, and the available domains, Figure 2f. Our development of the thermodynamic formulation on heterogeneous nucleation on fractal surfaces in the present study shows the rigorous results that recover the data in ref 14. In addition, we show how the fractal dimension and apparent contact angle affect the nucleation process and present the deviation extents of the critical size of embryos and nucleation energy barrier on the fractal surface from the smooth surface. Our results reveal that the formulas for the classic heterogeneous nucleation on the smooth surface can be used to approach the nucleation process on the fractal surface for the nonwetting case. For the wetting case, however, the classic approach is not valid anymore, and fractal surfaces can cause significant reduction or elimination of the critical embryo size and the required energy barrier.

We have also noticed some results in the literature different from the conclusions in the present study. For example, Fujii and Hirayama[6] reported that compared with the conventionally siliconized surface, the superwater-repellent fractal surface can heavily increase the size of the crystals but markedly decrease the number of crystals. The difference is due to the fact that the measured crystals in ref 6 are macrocrystals grown after 2 weeks, rather than the critical embryos. Yamamoto et al.[49] observed that alteration of the fractal dimension of lotus leaves can significantly change the apparent contact angle of the droplets, which is somewhat different than the results by the developed theory. This difference does not indicate that our results are wrong because the contact angle changes on lotus leaves reported in ref 49 are due to the removal of needle-shaped wax tubes, rather than a simple change of fractal dimension. Literature surveying also indicated significant changes of the contact angle when the substrate flat surfaces are replaced by the fractal surfaces for both the hydrophilic and hydrophobic solutions.[44−46,50] The liquid drops used are significantly beyond the fractal regions, and thus the results, as expected, deviate from the present study. Basically, the contact angle measurements or simulations on fractal surfaces in refs 44−46 and 50 are different than heterogeneous nucleation on fractal surface in the scenes of physics.

EXPLANATION OF VANISHING OF NUCLEATION ENERGY BARRIER IN THE REGIONS OF SMALL APPARENT CONTACT ANGLES

From the analysis in the previous sections, we have noticed the significant differences of the characteristics of heterogeneous nucleation on the fractal surfaces compared to those on the smooth or geometric conditioned surfaces in the literature:[9−11,13] the elimination of the nucleation energy barrier in the region of small apparent contact angles as shown in Figure 3. The results are also supported by the observation that the critical size of the embryos required for further growth decreases to zero in the contact angle region; see Figure 2. Another important fractal-dimension-and-contact-angle affected feature for nucleation is a maximum depth of an embryo from the top of the spherical-cap nucleus to the mimic contact planar shown in Figure 1. The maximum depth, H, can be given by

$$H = R_c(1 - \cos\theta) = R_{c0}h(\theta, D)(1 - \cos\theta) \quad (18)$$

Figure 4 plots the depth ratio, H/R_{c0}, as a function of θ as D increases from 2 to 3. Again, the depth ratio of a nonwetting

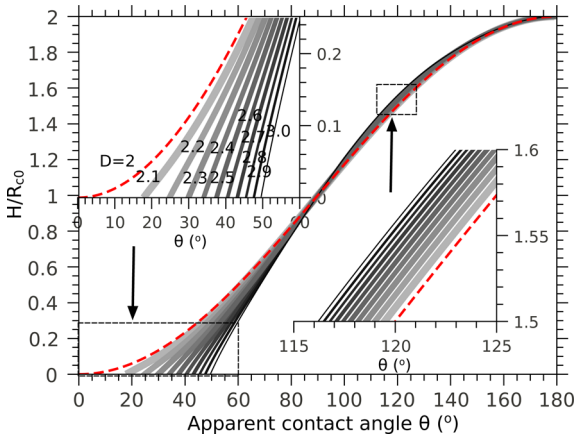

Figure 4. Plots of H/R_{c0} against θ as fractal dimension changes from 2 to 3.

nucleus in contact with the fractal surface remains, showing approximate values with the case of the smooth surface. And also the depth ratio of a very wetting nucleus in contact with the fractal surface vanishes owing to the failure of forming a spherical-cap nucleus on the fractal surface.

While we have shown the free energy required for forming a nucleus of the very wetting phase on a fractal surface reduces to zero, implying the possibilities of spontaneous crystallization (or condensation), it remains unclear how this process takes place and the hidden mechanisms result in the observations above. We first envision a rough surface structured in a fractal and a smooth surface where the same number of molecules of the bulk phase 1 are assembled together to form the crystal phase 2, as illustrated in Figure 5. Since it is a schematic demonstration, we would not intend to present specific crystal structures. The molecules that are aggregated together forming a spherical-cap nucleus on the smooth surface, however, may

DOI: 10.1021/acs.jpcc.5b07709
J. Phys. Chem. C 2015, 119, 27426−27433

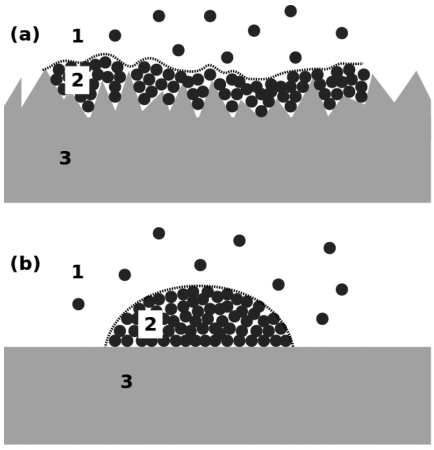

Figure 5. Schematic illustration of the patterns of the wetting nucleation process with which the embryo phase 2 is in contact with the substrate phase 3 of (a) a fractal surface and (b) a smooth surface.

settle on the fractal surface without the defined geometry; see Figure 5a. So it is not possible to identify the apparent contact angle by the Wenzel equation, and consequentially, eq 17 fails to describe the relative energy barrier against forming embryos for the very wetting case. On the other hand, even the spherical-cap shape holds for the very wetting nucleus; it may generate physical problems for the critical size and depth. For example, with R_{c0} = 30 nm, θ = 43.5°, and D = 2.7 for typical silica porous material,[7] the estimated critical embryo radius is about 1.1 nm, only 3 times the diameter of a water molecule, and the estimated depth H is about 0.3 nm, the diameter of a water molecule. Both the estimated embryo size and depth for such a wetting case are not likely to occur in practice. It also should be pointed out that as in refs 11 and 13 the characteristics of heterogeneous nucleation on the fractal surfaces discussed are limited to where the classic surface physic laws (e.g., the Young and Wenzel equations) will approximately apply. A few layers of molecules on solid substrate, as exemplified in Figure 5a, may not hold the classic surface physics laws. We should also note the influences of the shape of the crystal embryos (cf. the ellipsoidal shape embryos[51]) and the wetting extent (cf. the Cassie−Baxter model for partially wet states of rough surface[50]). As a result, the nucleation of embryos with very tiny size on fractal surfaces may be beyond the developed thermodynamic formulas based on the classic thermodynamics, and the relevant issues deserve rigorous study in the future (e.g, molecular dynamics simulations[52]). However, if the fractal structure of a surface can significantly decrease the energy barrier of forming a nucleation embryo or enhance the spread of liquid, practical approaches in fabricating superheterogneous nucleation surface, like the superwetting surface indicated by Drelich and Chibowski,[53] are through manipulation of surface texture with fractal structure.

CONCLUSION

In the present study, we aimed to clarify the principles of heterogeneous nucleation on fractal surfaces and understand how the fractal nature of the substrate surfaces influence the characteristics of the heterogeneous nucleation process. The study consisted of development of a thermodynamic model from the change of Gibb free energy as nucleation takes place, analyzing the featured parameters that are distinct from the classic nucleation on flat surfaces, and proposing a mechanism that is possible to explain the abnormality of the shape function in the regions of low apparent contact angles. The conclusions from this study are summarized as follows: (1) A thermodynamic model was developed to capture the heterogeneous nucleation on fractal surfaces. We reported two important parameters to characterize the nucleation process on the fractal surfaces: the critical embryo size coefficient, $h(\theta, D)$, and the shape function, $f(\theta, D)$. We also obtained the explicit expressions of $h(\theta, D)$ and $f(\theta, D)$ that are the functions of θ and D for the first time. (2) We reported the available domains for forming critical nucleation embryos, that is, $h(\theta, D) > 0$ and $\partial^2\Delta G/\partial R^2|_{R=R_c} < 0$, and found that the domains change with the fractal dimension. (3) We found significant deviations of the values of $h(\theta, D)$ on the fractal surfaces from those on the flat surfaces as θ is acute, while the deviations become negligible as θ is right and/or obtuse. (4) The values of shape function, $f(\theta, D)$, are similar to those of $h(\theta, D)$. The results showed that the energy barrier resistance against forming nuclei in critical size could reduce to zero, revealing that nucleation on a fractal surface can take place spontaneously as θ is relatively small. (5) The wetting nucleation embryos of the very tiny size on fractal surfaces predicted by the developed thermodynamic model could be false because of the limitation of the Wenzel approach, and the relevant issues deserve rigorous study in the future.

AUTHOR INFORMATION

Corresponding Author

*E-mail: cengq14@zju.edu.cn. Phone: +86-0571-8820-6763.

Notes

The authors declare no competing financial interest.

ACKNOWLEDGMENTS

This research is supported by the National Natural Science Foundation of China (No. 51408536) and China National Major Fundamental Research Grant (973 Program, No. 2013CB035901).

REFERENCES

(1) Schutzius, T. M.; Jung, S.; Maitra, T.; Eberle, P.; Antonini, C.; Stamatopoulos, C.; Poulikakos, D. Physics of Icing and Rational Design of Surfaces with Extraordinary Icephobicity. *Langmuir* **2015**, *31*, 4807−4821.

(2) Heydari, G.; Thormann, E.; Jarn, M.; Tyrode, E.; Claesson, P. M. Hydrophobic Surfaces: Topography Effects on Wetting by Supercooled Water and Freezing Delay. *J. Phys. Chem. C* **2013**, *117*, 21752−21762.

(3) Mishchenko, L.; Hatton, B.; Bahadur, V.; Taylor, J. A.; Krupenkin, T.; Aizenberg, J. Design of Ice-free Nanostructured Surfaces Based on Repulsion of Impacting Water Droplets. *ACS Nano* **2010**, *4*, 7699−7707.

(4) Alizadeh, A.; Yamada, M.; Li, R.; Shang, W.; Otta, S.; Zhong, S.; Ge, L.; Dhinojwala, A.; Conway, K. R.; Bahadur, V.; Vinciquerra, A. J.; Stephens, B.; Blohm, M. L. Dynamics of Ice Nucleation on Water Repellent Surfaces. *Langmuir* **2012**, *28*, 3180−3186.

(5) Jacobsen, S.; Scherer, G. W.; Schulson, E. M. Concrete−ice Abrasion Mechanics. *Cem. Concr. Res.* **2015**, *73*, 79−95.

(6) Fujii, I.; Hirayama, N. Use of Super-water-repellent Fractal Surfaces in The Crystallization of Macromolecules. *Acta Crystallogr., Sect. D: Biol. Crystallogr.* **1999**, *55*, 1247−1249.

(7) Stolyarova, S.; Saridakis, E.; Chayen, N.; Nemirovsky, Y. A Model for Enhanced Nucleation of Protein Crystals on a Fractal Porous Substrate. *Biophys. J.* **2006**, *91*, 3857−3863.

DOI: 10.1021/acs.jpcc.5b07709
J. Phys. Chem. C 2015, 119, 27426−27433

(8) Liu, Y.-X.; Wang, X.-J.; Lu, J.; Ching, C.-B. Influence of the Roughness, Topography, and Physicochemical Properties of Chemically Modified Surfaces on the Heterogeneous Nucleation of Protein Crystals. *J. Phys. Chem. B* **2007**, *111*, 13971−13978.
(9) Fletcher, N. H. Size Effect in Heterogeneous Nucleation. *J. Chem. Phys.* **1958**, *29*, 572−576.
(10) Liu, X. Effect of Foreign Particles: a Comprehensive Understanding of 3D Heterogeneous Nucleation. *J. Cryst. Growth* **2002**, *237*−*239*, 1806−1812.
(11) Qian, M.; Ma, J. Heterogeneous Nucleation on Convex Spherical Substrate Surfaces: A Rigorous Thermodynamic Formulation of Fletcher's Classical Model and the New Perspectives Derived. *J. Chem. Phys.* **2009**, *130*, 214709.
(12) Qian, M. Heterogeneous Nucleation on Potent Spherical Substrates During Solidification. *Acta Mater.* **2007**, *55*, 943−953.
(13) Qian, M.; Ma, J. The Characteristics of Heterogeneous Nucleation on Concave Surfaces and Implications for Directed Nucleation or Surface Activity by Surface Nanopatterning. *J. Cryst. Growth* **2012**, *355*, 73−77.
(14) Wang, M.; Zhang, Y.; Zheng, H.; Lin, X.; Huang, W. Investigation of the Heterogeneous Nucleation on Fractal Surfaces. *J. Mater. Sci. Technol.* **2012**, *28*, 1169−1174.
(15) Zhang, Y.; Wang, M.; Lin, X.; Huang, W. Effect of Substrate Surface Microstructure on Heterogeneous Nucleation Behavior. *J. Mater. Sci. Technol.* **2012**, *28*, 67−72.
(16) Mu, C.; Pang, J.; Lu, Q.; Liu, T. Effects of Surface Topography of Material on Nucleation Site Density of Dropwise Condensation. *Chem. Eng. Sci.* **2008**, *63*, 874−880.
(17) Liu, T.; Sun, W.; Li, X.; Sun, X.; Ai, H. Growth Modes of Condensates on Nano-textured Surfaces and Mechanism of Partially Wetted Droplet Formation. *Soft Matter* **2013**, *9*, 9807−9815.
(18) Zeng, Q.; Li, K.; Fen-Chong, T. Heterogeneous Nucleation of Ice from Supercooled NaCl Solution Confined in Porous Cement Paste. *J. Cryst. Growth* **2015**, *409*, 1−9.
(19) Meuler, A. J.; McKinley, G. H.; Cohen, R. E. Exploiting Topographical Texture to Impart Icephobicity. *ACS Nano* **2010**, *4*, 7048−7052.
(20) Holbrough, J. L.; Campbell, J. M.; Meldrum, F. C.; Christenson, H. K. Topographical Control of Crystal Nucleation. *Cryst. Growth Des.* **2012**, *12*, 750−755.
(21) Qi, Y.; Klausner, J. F.; Mei, R. Role of Surface Structure in Heterogeneous Nucleation. *Int. J. Heat Mass Transfer* **2004**, *47*, 3097−3107.
(22) Zhang, X.-X.; Chen, M.; Fu, M. Impact of Surface Nanostructure on Ice Nucleation. *J. Chem. Phys.* **2014**, *141*, 124709.
(23) Campbell, J. M.; Meldrum, F. C.; Christenson, H. K. Is Ice Nucleation from Supercooled Water Insensitive to Surface Roughness? *J. Phys. Chem. C* **2015**, *119*, 1164−1169.
(24) Stolyarova, S.; Baskin, E.; Chayen, N. E.; Nemirovsky, Y. Possible Model of Protein Nucleation and Crystallization on Porous Silicon. *Phys. Status Solidi A* **2005**, *202*, 1462−1466.
(25) Stolyarova, S.; Baskin, E.; Nemirovsky, Y. Enhanced Crystallization on Porous Silicon: Facts and models. *J. Cryst. Growth* **2012**, *360*, 131−133.
(26) Ono, Y.; Mayama, H.; Furó, I.; Sagidullin, A. I.; Matsushima, K.; Ura, H.; Uchiyama, T.; Tsujii, K. Characterization and Structural Investigation of Fractal Porous-silica Over An Extremely Wide Scale Range of Pore Size. *J. Colloid Interface Sci.* **2009**, *336*, 215−225.
(27) Zeng, Q.; Li, K.; Fen-Chong, T.; Dangla, P. Surface Fractal Analysis of Pore Structure of High-Volume Fly-ash Cement Pastes. *Appl. Surf. Sci.* **2010**, *257*, 762−768.
(28) Zeng, Q.; Luo, M.; Pang, X.; Li, L.; Li, K. Surface Fractal Dimension: An Indicator to Characterize the Microstructure of Cement-based Porous Materials. *Appl. Surf. Sci.* **2013**, *282*, 302−307.
(29) Mandelbrot, B. B. *The Fractal Geometry of Nature*; WH Freeman and Co.: New York, 1983.
(30) Sen, S.; Mukerji, T. A Generalized Classical Nucleation Theory for Rough Interfaces: Application in the Analysis of Homogeneous Nucleation in Silicate Liquids. *J. Non-Cryst. Solids* **1999**, *246*, 229−239.
(31) Roldugin, V.; Tikhonov, N. Heterogeneous Nucleation on Fractal Surfaces. *Dokl. Phys. Chem.* **2002**, *383*, 84−87.
(32) Bottiglione, F.; Carbone, G. Role of Statistical Properties of Randomly Rough Surfaces in Controlling Superhydrophobicity. *Langmuir* **2013**, *29*, 599−609.
(33) Grzelak, E. M.; Errington, J. R. Nanoscale Limit to the Applicability of Wenzel's Equation. *Langmuir* **2010**, *26*, 13297−13304.
(34) Nosonovsky, M. On the Range of Applicability of the Wenzel and Cassie Equations. *Langmuir* **2007**, *23*, 9919−9920.
(35) Gao, L.; McCarthy, T. J. How Wenzel and Cassie Were Wrong. *Langmuir* **2007**, *23*, 3762−3765.
(36) McHale, G. Cassie and Wenzel:âĂ Were They Really So Wrong? *Langmuir* **2007**, *23*, 8200−8205.
(37) Marmur, A.; Bittoun, E. When Wenzel and Cassie Are Right: Reconciling Local and Global Considerations. *Langmuir* **2009**, *25*, 1277−1281.
(38) Erbil, H. Y.; Cansoy, C. E. Range of Applicability of the Wenzel and CassieâĹŠBaxter Equations for Superhydrophobic Surfaces. *Langmuir* **2009**, *25*, 14135−14145.
(39) Bogdan, A. Thermodynamics of The Curvature Effect on Ice Surface Tension and Nucleation Theory. *J. Chem. Phys.* **1997**, *106*, 1921−1929.
(40) Hienola, A. I.; Winkler, P. M.; Wagner, P. E.; Vehkamaki, H.; Lauri, A.; Napari, I.; Kulmala, M. Estimation of Line Tension and Contact Angle From Heterogeneous Nucleation Experimental Data. *J. Chem. Phys.* **2007**, *126*, 094705.
(41) Ward, C.; Levart, E. Conditions for Stability of Bubble Nuclei in Solid Surfaces Contacting a Liquid-gas Solution. *J. Appl. Phys.* **1984**, *56*, 491−500.
(42) McGaughey, A.; Ward, C. Droplet Stability in a Finite System: Consideration of The Solid-vapor Interface. *J. Appl. Phys.* **2003**, *93*, 3619−3626.
(43) Forest, T.; Ward, C. Homogeneous Nucleation of Bubbles in Solutions at Pressures above The Vapor Pressure of The Pure Liquid. *J. Chem. Phys.* **1978**, *69*, 2221−2230.
(44) Shibuichi, S.; Yamamoto, T.; Onda, T.; Tsujii, K. Super Water- and Oil-Repellent Surfaces Resulting from Fractal Structure. *J. Colloid Interface Sci.* **1998**, *208*, 287−294.
(45) Shibuichi, S.; Onda, T.; Satoh, N.; Tsujii, K. Super Water-Repellent Surfaces Resulting from Fractal Structure. *J. Phys. Chem.* **1996**, *100*, 19512−19517.
(46) Onda, T.; Shibuichi, S.; Satoh, N.; Tsujii, K. Super-Water-Repellent Fractal Surfaces. *Langmuir* **1996**, *12*, 2125−2127.
(47) Feng, L.; Li, S.; Li, Y.; Li, H.; Zhang, L.; Zhai, J.; Song, Y.; Liu, B.; Jiang, L.; Zhu, D. Super-Hydrophobic Surfaces: From Natural to Artificial. *Adv. Mater.* **2002**, *14*, 1857−1860.
(48) Wolansky, G.; Marmur, A. Apparent contact angles on rough surfaces: the Wenzel equation revisited. *Colloids Surf., A* **1999**, *156*, 381−388.
(49) Yamamoto, M.; Nishikawa, N.; Mayama, H.; Nonomura, Y.; Yokojima, S.; Nakamura, S.; Uchida, K. Theoretical Explanation of the Lotus Effect: Superhydrophobic Property Changes by Removal of Nanostructures from the Surface of a Lotus Leaf. *Langmuir* **2015**, *31*, 7355−7363.
(50) Kang, H. C.; Jacobi, A. M. Equilibrium Contact Angles of Liquid Droplets on Ideal Rough Solids. *Langmuir* **2011**, *27*, 14910−14918.
(51) Lubarda, V. A.; Talke, K. A. Analysis of the Equilibrium Droplet Shape Based on an Ellipsoidal Droplet Model. *Langmuir* **2011**, *27*, 10705−10713.
(52) Lauricella, M.; Meloni, S.; English, N. J.; Peters, B.; Ciccotti, G. Methane Clathrate Hydrate Nucleation Mechanism by Advanced Molecular Simulations. *J. Phys. Chem. C* **2014**, *118*, 22847−22857.
(53) Drelich, J.; Chibowski, E. Superhydrophilic and Superwetting Surfaces: Definition and Mechanisms of Control. *Langmuir* **2010**, *26*, 18621−18623.

DOI: 10.1021/acs.jpcc.5b07709
J. Phys. Chem. C 2015, 119, 27426−27433